ELSEVIER

Laboratory note

Action mechanisms and structure–activity relationships of PI3Kγ inhibitors on the enzyme: a molecular modeling study

R.-R. Kuang [a], F. Qian [a], Z. Li [b], D.-Z. Wei [a,*], Y. Tang [c,*]

[a] *State Key Laboratory of Bioreactor Engineering, New World Institute of Biotechnology, 130 Mei-Long Road, Shanghai 200237, China*
[b] *Institute of Pesticides and Pharmaceuticals, 130 Mei-Long Road, Shanghai 200237, China*
[c] *School of Pharmacy, East China University of Science and Technology, 130 Mei-Long Road, Shanghai 200237, China*

Abstract

Action mechanisms of four types of PI3Kγ inhibitors were investigated on the ligand-binding pocket (LBP) of PI3Kγ with molecular modeling method. At first five compounds whose complex structures with PI3Kγ were available experimentally were used to validate the reliability of docking program Autodock3.0. The results demonstrated that the program could reproduce the bound conformations of those compounds in crystal structures. Then the program was used to dock all the four types of PI3Kγ inhibitors into the LBP of the enzyme. The predicted activities of these compounds were in agreement with their experimental activities, and a pharmacophore model was hence derived for these compounds, which consisted of one hydrophobic portion flanked by two symmetric hydrophilic portions. Furthermore, the structure–activity relationships of PI3Kγ inhibitors were elucidated and the activity differences between them were discussed.
© 2006 Elsevier SAS. All rights reserved.

Keywords: PI3Kγ; Molecular docking; Pharmacophore; Structure–activity relationships

1. Introduction

Phosphoinositide 3-kinases (PI3Ks) catalyze the phosphorylation of 3-OH group of phosphatidyl myo-inositol (PtdIns) lipids to generate different 3′-phosphorylated lipid products that act as secondary messengers. PI3Ks are found to play important roles in a lot of biological processes, such as cell survival and proliferation, cell motility and adhesion, cytoskeletal rearrangement and vesicle trafficking [1,2]. There are three major classes of PI3Ks, namely Class I, II and III, based on their sequences and substrate specificities. Class I PI3Ks are further divided into Class IA and IB according to regulatory subunit. Class IA enzymes (α, β, and δ) have a p85 regulatory subunit containing two SH2 domains, whereas Class IB enzyme (PI3Kγ) has a p101 subunit, which is required for maximal Gβγ-stimulated formation of PIP$_3$ [3,4].

Macrophages and neutrophils from PI3Kγ knockout mice show reduced motility in vitro and in vivo models of inflammation, as well as an impaired respiratory burst [5–7]. PI3Kγ-deficient mice also show resistance to thromboembolism [8]. In addition, the lipid products resulting from PI3Kγ activity are elevated in certain tumors [9,10]. PI3Kγ/Akt signaling pathway not only involves in characteristic cancer processes but also contributes to resistance to chemotherapy and γ-irradiation therapy [11]. All these facts suggest that PI3Kγ is a potential target for cancer and inflammation treatments, and hence, spark great interests in the discovery and development of its inhibitors.

Docking method is a powerful tool to explore ligand-receptor interaction providing 3D structure of the target. Currently docking software mainly includes Autodock, Dock, FlexX and Gold [12–15]. Here Autodock was used for the study. Autodock uses three types of algorithms (Genetic Algorithm, SW algorithm and Lamarckian Genetic Algorithm) to place ligand into the active site of a target [12]. The scoring function of Autodock is used to estimate the free binding energy of the ligand-protein complex. Normally Autodock provides 10 can-

didate conformations. Among them the conformation with the lowest binding energy could be regarded as the bound conformation to protein.

Program Grid22 is a computational procedure to determine energetically favorable binding sites on molecules with known structures [16]. The program works by defining a three-dimensional grid of points that contains the chosen ligand-binding pocket. The interaction of the Probe groups with the target is computed at sample positions (the grid points) distributed throughout and around the molecule. With the Probe at each Grid point in turn, the interaction is calculated from: $E_{total} = \sum E_{LJ} + \sum E_{HB} + \sum E_Q + S$, where E_{total}, E_{LJ}, E_{HB}, E_Q and S represent overall energy, Lennard–Jones interaction, hy-

drogen-bonding interaction, electrostatic interaction and entropic term, respectively.

In the last decade, four types of PI3Kγ inhibitors (benzopyrano, quinazoline, quinoline and caffeine analogs [17–21]) have been discovered, shown in Fig. 1. The first three types of compounds have a benzopyrano, quinazoline and quinoline moiety, respectively, and the last one is derived from caffeine. However, there are some common weaknesses for these inhibitors, such as low activities, low selectivity and low water-solubility. Therefore, it is necessary to explore the structure–activity relationships of known ligands and their action mechanisms on the enzyme in order to shed light on the search of new potent, selective and well water-soluble PI3Kγ inhibitors.
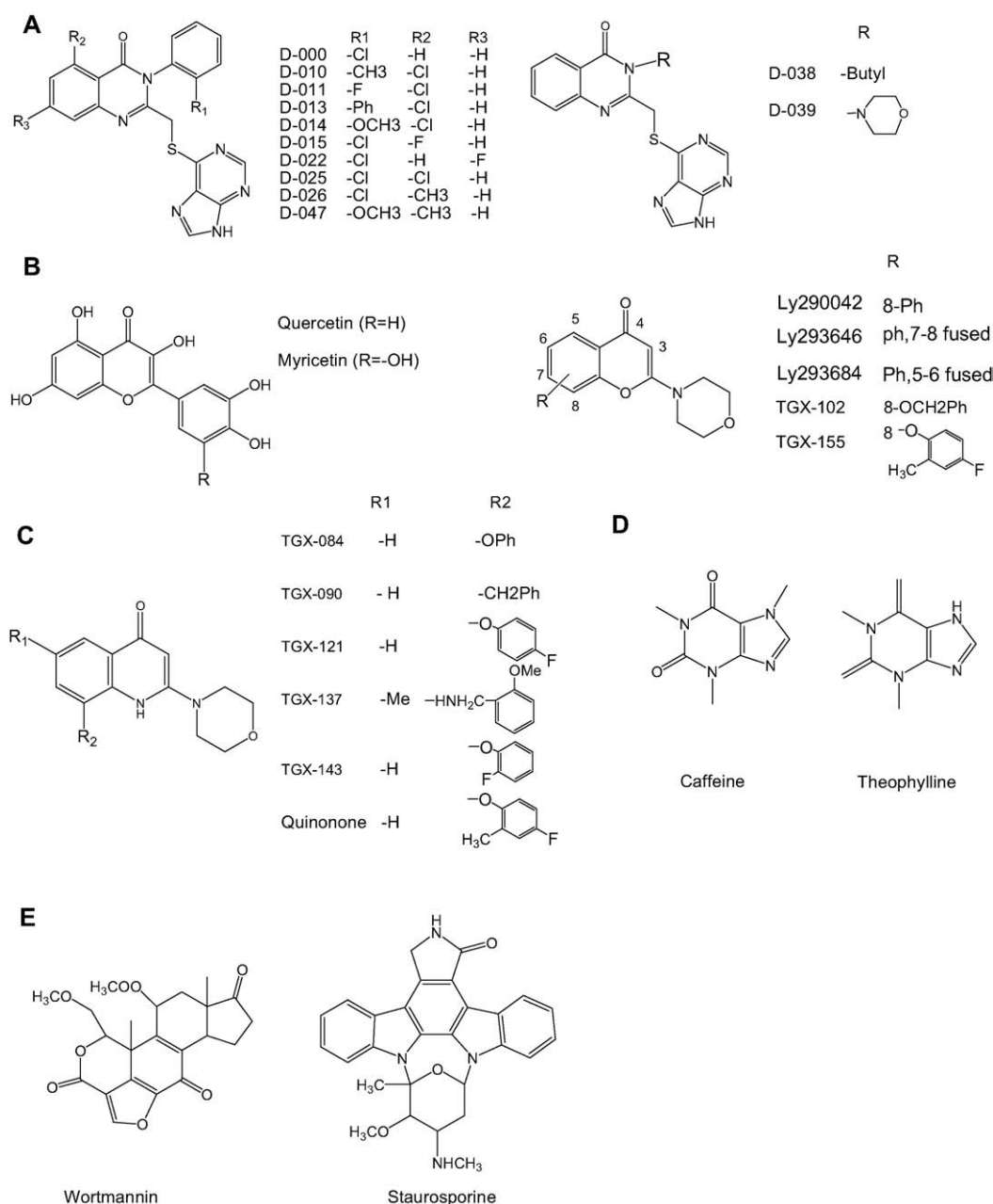

Fig. 1. Structures of 29 PI3Kγ inhibitors used in the study. (A) Quinazoline derivatives, (B) Benzopyrano derivatives, (C) Quinoline derivatives, (D) Caffeine analogs, (E) Wortmannin and Staurosporine.

To date, six X-ray crystal structures of PI3Kγ complexed with ligands have been reported [22]. The ligands include ATP, wortmannin, Ly294002, quercetin, myricetin, and staurosporine. All these ligands bind to the enzyme at the same place regarded as the ligand-binding pocket (LBP). From these structures we also learnt that PI3Kγ shares some common structural features with other kinases, such as ATP-binding site and total structure similarity. In this paper we conducted a molecular modeling study to investigate the interactions between PI3Kγ and those known inhibitors, then to generate a pharmacophore model for them and analyze the structure–activity relationships of those inhibitors with Autodock and Grid.

2. Materials and methods

2.1. Preparation of enzyme

The X-ray crystal structure of PI3Kγ complexed with Ly290042 was retrieved from the Protein Data Bank [23], entry code 1E7V. After removing the bound ligand and water molecules, the enzyme was treated with AutoDockTools so that it could be used in subsequent Autodock study. All residues enclosed within a sphere of 6Å radius around the bound ligand were defined as the ligand-binding pocket.

2.2. Preparation of ligands

Total 29 synthetic and natural compounds (shown in Fig. 1) from the four types of inhibitors were used in the study. The inhibitive activities of 25 compounds on PI3Kγ, expressed as IC_{50}, and the corresponding $-LogIC_{50}$, were listed in Table 1. Their 3D structures were constructed with Accelrys software Cerius2 version 4.8 [24], followed by energy minimization with Polak-Ribiere method and conjugate gradient method to a root mean square (RMS) energy gradient of 0.1 kcal/(mol Å^2). CVFF force field and Gasteiger charges were employed throughout the article.

2.3. Docking

Autodock3.0 program was used for molecular docking and scoring. All rotatable bonds of each molecule were considered in the docking process to identify the possible binding conformation of the inhibitors with PI3Kγ. The number of grid points in xyz was set to 90, 90, 90, the spacing value equivalent to 0.375 Å, and the $N\alpha$ atom of Lys833 regarded as grid center. During docking, the number of individuals in population, maximum number of energy evaluation, maximum number of generations and GA-LS runs were rectified to 150, 3,000,000, 2,700,000 and 10, respectively. Other parameters were default value implemented by the program.

2.4. Grid

Grid22 was employed to calculate binding energies between probes and macromolecule with a 22 × 24 × 23 Å cage con-

Table 1
Biological activities of 25 inhibitors

Serial number	Inhibitors	IC_{50} μM[a]	$-LogIC_{50}$
1	D-000	7.7	5.11
2	D-010	0.7	6.15
3	D-011	1.0	6.00
4	D-015	3.6	5.44
5	D-022	40	4.40
6	D-025	1.5	5.82
7	D-026	1.7	5.77
8	D-038	60	4.22
9	D-047	0.5	6.30
10	Ly294002	2	5.70
11	TGX-084	5	5.30
12	TGX-102	3	5.52
13	TGX-121	5	5.30
14	TGX-155	5	5.30
15	Quercetin	3.8	5.42
16	Myricetin	1.3	5.89
17	Quinolone	5	5.30
18	Theophlline	800	3.10
19	Caffeine	1000	3.00
20	D-013	2.1	5.68
21	D-014	0.56	6.25
22	D-039	38	4.42
23	TGX-90	3	5.52
24	TGX-137	2.95	5.53
25	TGX-143	2	5.70

[a] IC_{50} equals the concentration of compound required to induce 50% of the maximum inhibition.

taining all of crucial residues to ligand binding [22], after the enzyme target was neutralized by adding potassium cations with Greater program included in Grid22. The main Grid runs were then carried out with a grid spacing of 0.25 Å. Non-bonded interaction energies between the protein and 40 probes were calculated. The 40 probes included 32 monoatomic and 8 polyatomic chemical groups and were comprehensive.

2.5. Analysis of results

All the docking results were visualized and analyzed with software Swiss-PdbViewer, i.e. Deep View [25].

3. Results and discussion

When the experimental structure of a protein is available, docking study is very helpful for understanding drug action mechanism on the protein and designing new ligand to act on the protein. Flexibility of small molecules usually is considered thoroughly in the docking procedure. However, flexibility of the protein is still considered very little. Therefore, docking quality is case-dependent and software-dependent, which means different software could lead to different docking results, and certain software is good in some cases, but bad in others. In this study, Autodock was selected as our docking tool. So, at first we should validate the docking results to make sure Autodock is suitable for this case. Then based on the Autodock results, we investigated the action mechanisms of all the four types of PI3Kγ inhibitors on the enzyme. Furthermore, we generated a pharmacophore model and elucidated the

structure–activity relationships of these inhibitors in combination with Grid results.

3.1. Validation of Autodock method

To validate the docking results, five known PI3Kγ inhibitors whose complex structures with the enzyme were available were served as a test set. These compounds were quercetin, myricetin, wortmannin, staurosporine and Ly290042. The results demonstrated that Autodock could reproduce those bound conformations in crystal structures very well. The RMS deviations for the heavy atoms were only 0.92, 1.2, 1.43, 1.22 and 1.31 Å for quercetin, myricetin, wortmannin, staurosporine and Ly290042, respectively, which indicated that the ability of Autodock3.0 to predict bound conformation of ligand was acceptable.

Furthermore, the first 19 synthetic and natural PI3Kγ inhibitors in Table 1 were used to evaluate if Autodock could predict the binding affinities of inhibitors quantitatively. These compounds were not very active, activities ranging from mM to μM, that's why we should try to find new potent inhibitors. Their docking scores (binding free energies) were shown in Table 2. A simple linear fit with partial least-squares (PLS) analysis was conducted to explore the relationship between the binding score and activity –LogIC$_{50}$ (Eq. (1)). As shown in Fig. 2 and Eq. (1), linear correlations existed between the binding scores and biological activities, which indicated that Autodock3.0 could quantitatively predict the biological activities of inhibitors and the linear model from the simple linear fit could be used in virtual screening toward PI3Kγ:

$$- \text{LogIC}_{50} = -4.134(\pm 0.825) - 0.994(\pm 0.087) \times \text{Binding core} \tag{1}$$

$$n = 19, \ R = 0.94, \ F = 129.95, \ S = 0.087$$

where N is the number of tested ligands, S.D. is the standard deviation, R is the correlation coefficient and F is a statistic variable.

To validate the linear model, we docked additional five inhibitors (TGX-90, TGX-137, TGX-143, D-013 and D-014, shown in Fig. 1) [19,20] into LBP of PI3Kγ. Binding energy

Table 2
The binding free energies of ligands with PI3Kγ. The binding free energies (kcal/mol) of the protein-ligand complex were estimated by the scoring function of Autodock 3.0

Inhibitors	$\Delta G_{binding}$	Inhibitors	$\Delta G_{binding}$
D-000	−9.49	TGX-084	−9.85
D-010	−9.84	TGX-102	−9.49
D-011	−10.21	TGX-121	−9.80
D-015	−9.73	TGX-155	−9.11
D-022	−9.12	Quercetin	−10.12
D-025	−9.87	Myricetin	−9.97
D-026	−9.94	Quinolone	−9.15
D-038	−8.75	Theophlline	−7
D-047	−10.42	Caffeine	−7.52
Ly294002	−10.12		

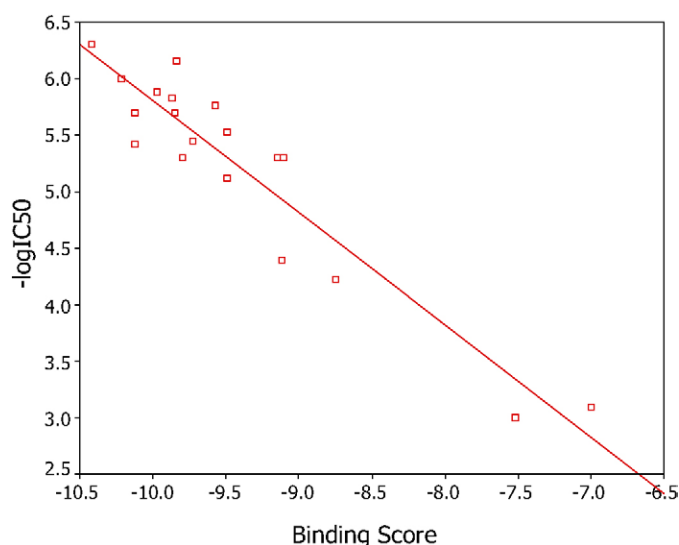Fig. 2. Relationship between binding score and –LogIC$_{50}$ value of inhibitors.

scores of those inhibitors were –8.80, –8.99, –9.77, –9.61 and –9.70 kcal/mol, respectively. Predicted -LogIC$_{50}$ values of the five compounds by Eq. (1) were listed in Table 3. From the table it was clear that the deviations between the predicted and experimental -LogIC$_{50}$ values were less than 0.92, which indicated that Eq. (1) could be applied to predict inhibitors' activities quantitatively. Thus the binding energy calculated by Autodock could instruct us how to rebuild structure of lead compounds.

3.2. Binding mode of quinazoline derivatives

Quinazoline derivatives are a major type of inhibitors of PI3Kγ. To explore the action mechanism of quinazoline derivatives on PI3Kγ, compound D-010 (Fig. 1) was chosen as a representative. The IC$_{50}$ value of D-010 was 0.5 μM on PI3Kγ [20]. The docking mode of D-010 with PI3Kγ provided a framework for understanding the structure–activity relationships that have been reported for D-010 and related derivatives. The bound conformation of D-010 on PI3Kγ was shown in Fig. 3a, superposed with that of ATP. The N_1 atom of purine moiety of D-010 formed a hydrogen bonding interaction with Nα atom of Lys833, and there was an additional hydrogen bond between the ketone moiety of D-010 and the carboxyl group of side chain of Asp964 (Fig. 4a). Occupying a similar space as the ribose of ATP and the 8-phenyl ring of Ly290042, the 3-phenyl ring of D-010 was located in a region that has

Table 3
Comparison of predicted –LogIC$_{50}$ values of the five inhibitors with experimental –LogIC$_{50}$ values of the five inhibitors and Q of the five inhibitors $Q = | - \text{LogIC}_{50 \text{predicted value}} - (- \text{LogIC}_{50 \text{ real value}})$

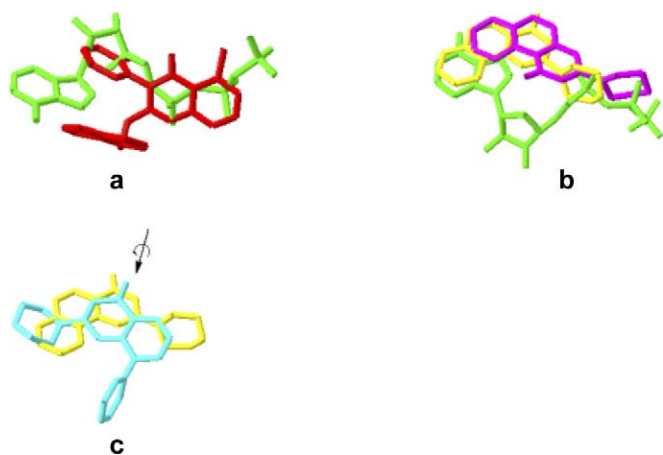| Inhibitors	–LogIC$_{50}$ predicted value	–LogIC$_{50 \text{ real}}$ value	Q
TGX-90	4.61	5.52	0.91
TGX-137	5.58	5.30	0.28
TGX-143	4.80	5.70	0.90
D-013	5.42	5.68	0.26
D-014	5.51	6.25	0.74

Fig. 3. (a) A comparison of binding model of D-010 to PI3Kγ active site with that of ATP. (b) A comparison of binding modes of Ly293646 (yellow), Ly293684 (pink) and ATP (green) in PI3Kγ active site. (c) Illustration of the relationships of the orientation of the chromone moieties of Ly293646 (yellow) and Ly290042 (azury). For each panel, the structures containing the compounds were superimposed on each other using the Cα coordinates of the enzyme.

been designated as hydrophobic region I in the protein kinases and packed against Met804, Trp812 on one side and Met953 on the other side. According to Walker [22], removal of the phenyl ring decreased inhibition approximately threefold, and biological activity data of D-010, D-038 and D-039 [20] proved the importance of 3-phenyl moiety. Structural examination of other protein kinases, including the c-AMP-dependent protein kinase and *c*-Src, suggested that the bulky 3-phenyl group of D-010 should be a specific feature for PI3Ks inhibitors [22]. The active site of PI3Kγ is more open at this position than those in other protein kinases, and PI3Kγ makes only limited contact with the ribose moiety of ATP. D-010 probably could not be well accommodated in other protein kinases that make more extensive interactions with the ribose and thus have less space in this region. According to Figs. 3a and 4a, the adenine ring of D-010 was also located in the hydrophobic region I, packing against Ile879, Tyr867 and Ile963 on one side and Met953 on the other side. The quinazoline ring of D-010 extended into a similar position (a hydrophilic region) to the bridging oxygen of α, β phosphates of ATP (Fig. 3a), which explained why D-010 inhibits PI3Kγ more effectively than other inhibitors.

D-022 is a potential inhibitor for PI3Kγ with an IC_{50} of 40 μM [20]. There was a hydrogen bond between N_9 atom of its purine moiety and amide group of the side chain of residue Lys833. Moreover, another hydrogen bond existed between the ketone moiety of D-022 and the carboxyl group on the side chain of residue Asp950 (Fig. 4a). D-022 has a fluorin atom at 7 position of quinazoline ring and no group at 5 position. Owing to steric hindrance the binding model of D-022 could not overlap with that of D-010. But its quinazoline ring was coplanar with that of D-010, and its 3-phenyl group paralleled to counterpart of D-010 (Fig. 4a). As shown in Fig. 4a, the whole molecule of D-022 was more adjacent to hydrophilic residues (such as Asp950, Asn951 and Thr887) than D-010, which caused the activity declination of D-022 because the 3-

phenyl, quinazoline and adenine ring can't well be in hydrophobic environment. If there weren't a little bulky group at 5 position, the activity would also decline due to the same reason. Above analysis demonstrated that the binding modes of quinazoline derivatives had similarity on the whole.

3.3. Binding modes of Ly293646 and Ly293684

Ly293646 and Ly293684 (Fig. 1) are two synthetic inhibitors for PI3Ks [18]. For the two inhibitors, their IC_{50} of 6 and 14 μM have been measured for class IA PI3K. For PI3Kγ, according to Autodock binding scores and Eq. (1) their IC_{50} might be 1.4 and 4.0 μM, respectively. In view of their specificity in structure, here we discussed their possible binding modes with PI3Kγ in order to attain more comprehensive information of LBP. Fig. 4b showed that the ketone moiety of Ly293646 formed two hydrogen bonds with the side chain of Tyr867 and backbond amide of residue Asp964. The 7,8-fused phenyl group of Ly293646 and adenine moiety of ATP was in the same plane and coplanar (Fig. 3b), while it was morpholine ring of Ly290042 that was at the same position with adenine ring of ATP [22]. The chromone moiety of Ly293646 in the PI3Kγ complex was flipped 180° relative to that of Ly290042 in the PI3Kγ complex, as shown in Fig. 3d. Fig. 4b showed that its naphthyl ring fitted into the hydrophobic region I and packed against residues Trp812, Ile879, Ile881, Val880 and Ile831 on one side, Tyr867, Phe961, Met953 and Ile963 on the other side. The morpholinyl group of Ly293646 extended into a similar position to the bridging oxygen of the α, β phosphates of ATP. In term of Ly293684, there were two hydrogen bonds between O atom of morpholine moiety and the carboxyl group on the side chain of residue Asp964 (Fig. 4c). As shown in Fig. 3b, the naphthalene rings of Ly293646 and Ly293684 were coplanar and partially overlapped each other. Compared with Ly293684, the naphthyl moiety of Ly293646 was more embedded into the hydrophobic region I, which might explain why Ly293646 inhibited PI3Kγ more effectively than Ly293684. The morpholine moiety of Ly293684 occupied a similar space to that β phosphate of ATP occupied in the PI3K/ATP complex. Because both 5,6-fused phenyl of Ly293684 and 7,8-fused phenyl of Ly293646 are rigid rings, their binding modes differed from that of Ly290042. Otherwise, their inhibitive activities would decline dramatically due to possible steric hindrance.

3.4. The pharmacophore model of PI3kγ inhibitors

From the 3D binding models of above-mentioned inhibitors to PI3Kγ, a pharmacophore model could be derived for PI3kγ inhibitors. As shown in Fig. 5a, it consisted of three components crucial to inhibitive activities, namely, a hydrophobic part flanked by two approximately symmetric hydrophilic parts (I, II), which formed hydrophobic and hydrophilic contacts with the corresponding hydrophobic and hydrophilic regions of the LBP of PI3Kγ. Taking D-010 as an example, its quinazoline moiety belonged to hydrophilic portion I of the pharma-
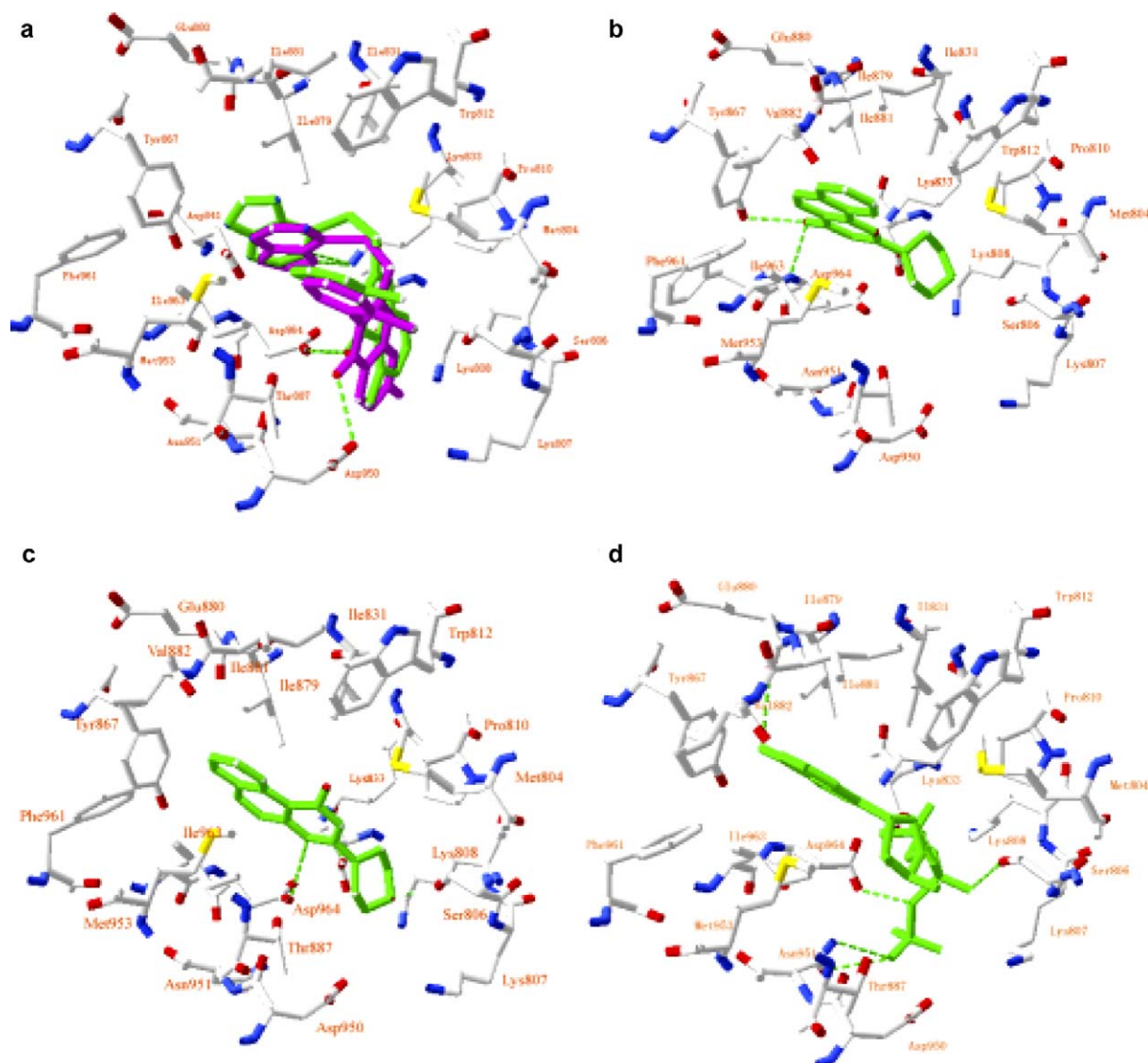
Fig. 4. Stereoplots of the active sites of the PI3K inhibitor complexes. Hydrogen bonds are shown as green dotted lines. (a) D-010 (green) and D-022 (pink), (b) Ly293646, (c) Ly293684, (d) ATP. The figure, together with Fig. 5, was prepared with Swiss-PdbViewer.

cophore while both phenyl and purine rings constituted the hydrophobic portion (Fig. 5b). The pharmacophore indicated that it was possible to design new potent PI3Kγ inhibitors with good water-solubility.

3.5. Structure–activity relationships

Furthermore, we explored the structure–activity relationships basing on binding modes of quinazoline derivatives and quercetin, and thus gained some indications on how to improve activities of these compounds. Analysis of binding modes of quinazoline derivatives with PI3Kγ indicated that 3, 5, 7 and 8 positions of quinazoline ring were very important to activity. Substitution of 3-phenyl by other groups decreased greatly hydrophobic interactions of these inhibitors with PI3Kγ and their selectivity for PI3Ks. In addition, 3-phenyl with C_1-C_3 carbon chain group strengthened the binding affinity of inhibitors. Removal of little bulky group at 5 position decreased the hydrophobic interactions of these inhibitors with PI3Kγ, while the bulky group increased repulsion between inhibitors and PI3Kγ and accordingly impaired their binding affinity. The 3D binding model of D-010 showed that there were Asp964, Asp836, Lys833, Lys807 and Lys808 by 7, 8 position of quinazoline ring. If group at 7, 8 position attracted vicinal residues such as Asp964 and Lys833 it would increase their activity, or it would cause phenyl, quinazoline and purine ring not to effectively take up hydrophobic environment because of steric hindrance with the side chains of Lys808 and Asp836, thereby decreases inhibitor's activity. It was also noted that group at 8 position sterically undermined inhibitor's activity more than group at 7 position. Meanwhile, examination of binding model of D-010 and its analogs suggested that group at 2 position of quinazoline ring should be lipophilic.

Grid is a useful tool helping us find out which chemical groups can bind hard to macromolecule. Using 40 probes including aromatic anionic carboxyl and sp^3 amine cation we em-
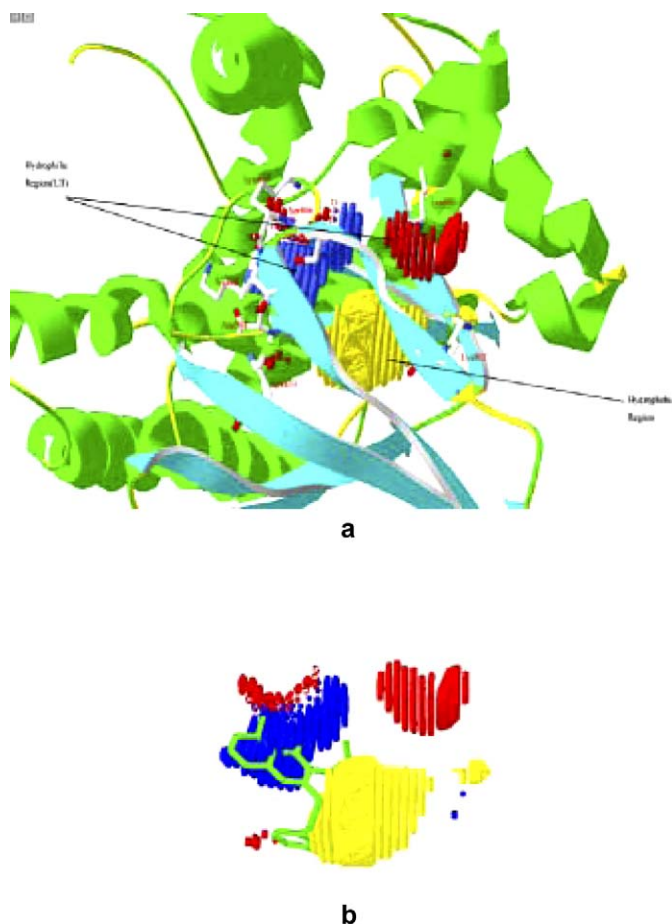
Fig. 5. (a) Ribbon diagram of the catalytic loop of PI3Kγ and stick illustration of the pharmacophore of PI3Kγ inhibitors in LBP. The pharmacophore includes three important parts, a hydrophobic region (yellow), hydrophilic regions I (blue) and II (red). (b) Superposition of binding conformation (green) of D-010 with the pharmacophore.

ployed Grid to scan the ligand-binding pocket of PI3Kγ and calculate the binding energy of those probes to PI3Kγ. The results of Grid demonstrated that there existed a negative and two positive positions in LBP of PI3Kγ. The negative position located by two residues, Asp964 and Asp836. One positive position located nearby residues Lys833, Lys808 and Lys807, the other nearby Lys890 and Lys802. According to Grid's instruction, addition of carboxyl, sulfonyl and amide at proper position of pharmacophore model must improve activity and water-solubility of PI3Kγ inhibitor with three above electrostatic positions in PI3Kγ active site utilized sufficiently. To the best of our knowledge, there is to date no reported inhibitor of PI3Kγ having carboxyl and amide on quinazoline and 3-phenyl ring. So introduction of carboxyl, sulfonyl and amide would further improve activities and water-solubility of quinazoline derivatives. Moreover, binding energies of halogen probes showed that different halogen interacted differently with PI3Kγ, and the bigger atom weight of halogen is, the stronger halogen binding affinity with PI3Kγ is. So iodine and bromine are favorable halogen in designing PI3Kγ inhibitor.

As to quercetin, the introduction of chemical group at 8 position would improve its selectivity for PI3Ks [22] and addition
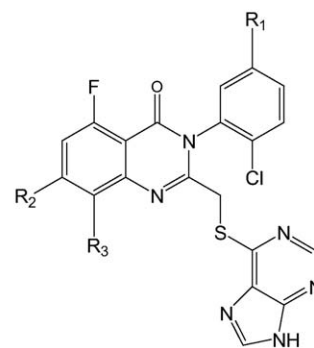
	R1	R2	R3
M1	- H	-COOH	- H
M2	- H	- H	- COOH
M3	- H	- NH$_2$	- H
M4	- H	- CH$_2$NH$_2$	- H
M5	- H	-guanidine	- H
M6	-CH$_2$COOH	- NH$_2$	- H
M7	-CH$_2$CH$_3$	- NH$_2$	- H
M8	-CH$_2$COOH	-COOH	- H

Fig. 6. Structures of eight designed compounds.

of carboxyl, sulfonyl or amide at 3′, 4′ position of 2-phenyl ring and 7 position of benzopyrano moiety would enforce its binding affinity with PI3Kγ, based on the X-ray crystallographic structure of quercetin/PI3Kγ and results of Grid. Likewise, introduction of carboxyl, sulfonyl or amide could be applied to analogues of quercetin. In a word, more hydrophobic and hydrophilic interactions with hydrophobic and hydrophilic regions of LBP, more electriferous groups ($-COO^-$, $-SO_3H^-$ and $-NH_3^+$) at proper position and better complementary shape match with PI3Kγ are the main reasons of higher binding affinity.

From above qualitative pharmacophore modeling and structure–activity relationship studies, we designed a list of inhibitors shown in Fig. 6 on the basis of quinazoline ring and predicted their biological activities (Table 4) according to Eq. (1). The table indicated that those designed compounds had better-predicted activities than existing quinazoline compounds, which made out that quantitative studies with Autodock corresponded to above qualitative analysis. Consequently, Autodock docking results can not only predict the relative binding affi-

Table 4
Predicted IC$_{50}$ of eight designed compounds by Eq. (1)

Designed compounds	Predicted IC$_{50}$ (μM)	Predicted -LogIC$_{50}$
M1	0.083	7.08
M2	0.310	6.51
M3	0.525	6.28
M4	0.331	6.48
M5	0.021	7.68
M6	0.081	7.09
M7	0.295	6.53
M8	0.020	7.71

nity of PI3Kγ inhibitors but also address their binding affinity differences in terms of interaction distributions.

4. Conclusion

In this paper, the binding modes of several types of PI3Kγ inhibitors were explored on the active site of the enzyme with program Autodock. The binding scores of these inhibitors from Autodock were found in accordance with their inhibitive activities, and hence the built linear model could be used to predict new designed compounds' activities quantitatively. Moreover, a pharmacophore model was generated for PI3Kγ inhibitors, and the structure–activity relationships of PI3Kγ inhibitors were discussed in combination with the analysis of Grid. These results could be helpful for designing new potent, selective and well water-soluble PI3Kγ inhibitors.

Acknowledgements

References

[1] B. Vanhaesebroeck, M.D. Waterfield, Exp. Cell Res. 253 (1999) 239–254.

[2] R.C. Stein, M.D. Waterfield, Mol. Med. Today 6 (2000) 347–357.

[3] L.R. Stephens, A. Eguinoa, H. Erdjument-Bromage, M. Lui, F. Cooke, J. Coadwell, A.S. Smrcka, M. Thelen, K. Cadwallader, P. Tempst, P.T. Hawkins, Cell 89 (1997) 105–114.

[4] S. Krugmann, P.T. Hawkins, N. Pryer, S. Braselmann, J. Biol. Chem. 274 (1997) 17152–17158.

[5] E. Hirsch, et al., Science 287 (2000) 1049–1053.

[6] Z. Li, et al., Science 287 (2000) 1046–1049.

[7] T. Sasaki, et al., Science 287 (2000) 1040–1046.

[8] E. Hirsch, et al., FASEB J. 15 (2001) 2019–2021.

[9] W.A. Phillips, et al., Cancer 83 (1998) 41–47.

[10] E.S. Gershtein, et al., Clin. Chim. Acta 287 (1999) 59–67.

[11] J. Angel Fresno Vara, E. Casado, J. de Castro, P. Cejas, Cancer Treat. Rev. 30 (2004) 193–204.

[12] G.M. Morris, D.S. Goodsell, R.S. Halliday, R. Huey, J. Comput. Chem. 19 (1998) 1639–1662.

[13] I.D. Kuntz, Science 257 (1992) 1078–1082.

[14] D. Hoffmann, B. Kramer, T. Washio, T. Steinmetzer, M. Rarey, T. Lengauer, JMC 42 (1999) 4422–4433.

[15] G. Jones, P. Willett, R.C. Glen, A.R. Leach, R. Taylor, J. Mol. Biol. 267 (1997) 727–748.

[16] P.J. Goodford, JMC 28 (1985) 849–857.

[17] F. William, Matter, Biochem. Biophy. Re. Com. 286 (1992) 624–631.

[18] J. Chris, J. Vlahos, Boil, Chem. 269 (1994) 5241–5248.

[19] A.J. Robertson, S. Jackson, V. Kenche, C. Yaip, H. Parbaharan, P. Thompson, International patent application 2001 [Patent number: WO 0153266 A1].

[20] C. Sadhu, K. Dick, J. Treiberg, C.G. Sowell, E.A. Kesicki, Oliver. A., International patent application.2001 [Patent number: WO 0181346 A2].

[21] C. Lazaros, N. Foukas, C. Daniele, Ktori, JBC 277 (2002) 37124–37130.

[22] H. Edward, Walker, Mol. Cell 6 (2000) 909–919.

[23] F.C. Bernstein, T.F. Koetzle, G.J. Williams, E.E. Meyer Jr., M.D. Brice, J.R. Rodgers, O. Kennard, T. Shimanouchi, M. Tasumi, J. Mol. Biol. 112 (1977) 535–542.

[24] Cerius2 4.8, Accelrys Inc, 1999.

[25] N. Guex, M.C. Peitsch, Electrophoresis 18 (1997) 2714–2723.